

A Numerical Comparison of Forced and Free Vibration of Circular Cylinders at Low Reynolds Number

J. S. Leontini¹, M. C. Thompson¹ and K. Hourigan¹

¹Department of Mechanical Engineering
Monash University, Victoria, 3800 AUSTRALIA

Abstract

Numerical simulations of flow past an elastically-mounted cylinder at $Re = 200$ have been performed, and the results directly compared to simulations of flow past a pure-tone driven oscillating cylinder at $Re = 200$. It is shown that the pure-tone driven oscillation can capture the important VIV characteristics, if the frequency and amplitude of oscillation are closely matched, for a limited range of U^* . Multi-frequency oscillation simulations have been performed in areas where the pure-tone oscillation is not accurate, and while they show a significant improvement in the lift force history, as yet they provide little improvement in values of phase.

Nomenclature	
A^*	Amplitude ratio, $\frac{y}{D}$
C_E	Energy transfer coefficient, $\int_T C_L \cdot U \cdot dt$
C_L	Lift coefficient, $\frac{F_L}{0.5\rho U^2 D}$
D	Cylinder diameter
F_L	Lift force / unit length
f	Oscillation frequency
f_N	Natural structural frequency
f_V	Vortex-shedding frequency from a stationary cylinder
m^*	Mass ratio, $\frac{m_{cyl}}{\frac{\pi}{4} D^2 \rho L}$
Re	Reynolds number, $\frac{UD}{\nu}$
St	Strouhal number, $\frac{f_V D}{U}$
t	Time, in seconds
T	Period of oscillation
U	Free-stream velocity
U^*	Reduced velocity, $\frac{U}{f_N D}$
v	Transverse cylinder velocity
y	Transverse cylinder displacement
ρ	Fluid density
ϕ_L	Phase between displacement and lift force (deg.)
ζ	Damping ratio, $\frac{c}{c_{crit}}$

Introduction

Vortex-induced vibration (VIV) of bluff structures can occur whenever a bluff body is immersed in a fluid stream. If the frequency of vortex shedding is close to the natural structural frequency of the structure, resonance can occur resulting in large-scale oscillations and ultimately structural failure.

Circular cylinders are extensively used in the study of bluff-body fluid dynamics, due to their geometrical simplicity and common use in engineering applications. Capitalising on these attributes, many vortex-induced vibration studies are based on a circular cylinder constrained to vibrate transverse to the free stream, such as the early investigation of Feng [8], and some more recent investigations ([11],[9]). While this system is greatly simplified, it contains the basic elements of coupled fluid-structure interaction.

In an attempt to better understand these systems, the fluid and structural systems are often decoupled. The cylinder can be

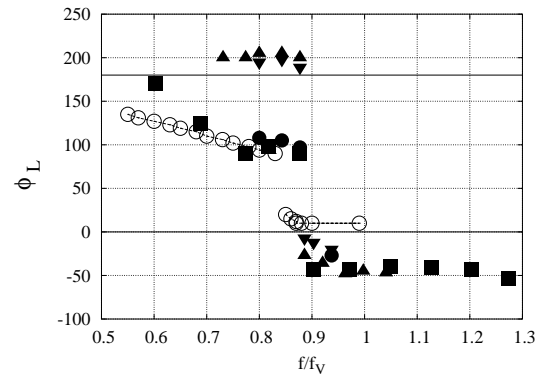


Figure 1: Phase vs frequency ratio f/f_V for pure-tone driven oscillation and VIV. ■ $A^* = 0.25$. ● $A^* = 0.4$. ▲ $A^* = 0.5$. ▼ $A^* = 0.6$. All driven oscillation data from [7] ○ VIV at high $m^* \zeta$, that produces peak amplitudes of ≈ 0.55 [9].

driven by some external force at a prescribed amplitude and frequency of sinusoidal oscillation. An extensive map of wake modes with varying amplitude and frequency has been created using this method [16].

While the results gained from driven oscillation experiments match the wake modes and phase difference between the cylinder displacement and lift force well, they do not predict observed levels of energy transfer C_E , where C_E is defined as the normalised work done by the fluid on the cylinder over a cycle of oscillation. This can be written as

$$C_E = \int_T C_L \cdot dy = \int_T C_L \cdot v \cdot dt, \quad (1)$$

where T is a period of oscillation, C_L is the lift coefficient and v is the cylinder velocity transverse to the free stream. If it is assumed the non-dimensionalised displacement and resulting lift force coefficient are pure sinusoids, such that $\frac{y(t)}{D} = A^* \sin(2\pi ft)$ and $C_L(t) = C_L \sin(2\pi ft + \phi_L)$, the energy transfer C_E only varies with the phase angle ϕ_L [5] such that

$$C_E = \pi C_L A^* \sin(\phi_L), \quad (2)$$

where A^* is the normalised cylinder displacement magnitude, $\frac{y}{D}$, and ϕ_L is the phase between the cylinder displacement and generated lift force. Inspection of equation 2 shows that C_E is positive whenever $0^\circ < \phi_L < 180^\circ$. This implies that in vortex-induced vibration ϕ_L always lies between these bounds, whereas during driven oscillation any values of ϕ_L are possible. Measurements of ϕ_L from VIV studies and driven oscillation studies are presented in figure 1.

Figure 1 shows that while the general trend of ϕ_L is the same between the VIV and driven oscillation cases, in that there is a

sudden drop in ϕ_L around $f/f_V = 0.9$, almost all of the driven oscillation cases have ϕ_L outside the range $0^\circ < \phi_L < 180^\circ$, predicting VIV should not occur. Only the lower amplitudes, $A^* = 0.25$ and $A^* = 0.40$, return a phase such that $0^\circ < \phi_L < 180^\circ$ at values of f/f_V below that at which the drop in ϕ_L occurs. However, it is known that VIV does occur at the higher A^* conditions ([11], [2]). It is clear from these results that while pure-tone driven oscillation captures many of the features of VIV, there are important flow features present during VIV that it does not re-create.

Any efforts to predict VIV using driven oscillation results have met with only mild success. One prediction [14] showed agreement between prediction and results over only a narrow range of flow speeds, and another [13] predicted an amplitude limit of $A_{MAX}^* = 1$, a limit later exceeded [10]. The prediction of VIV response from driven oscillation experiments has been investigated over a period of nearly 30 years, and has so far only yielded these mildly successful results. It is for this reason that a more complete driven oscillation model is required.

It is natural that the lower Re two-dimensional case should be used as a base case, to allow the physics of these flows to be understood. However, due to the practical difficulties of controlling such a low speed experiment, practically no experimental investigations of VIV have been made at $Re < 200$ ([1] is an exception). However, many numerical results are available ([4], [2]), that compare well to the limited experimental results. Experimental driven oscillation results at $Re < 200$ have been obtained [12], as well as numerical results ([4], [3]). While a phase change similar to that observed at higher Re has been reported, the phase at these lower Re is that between the cylinder displacement and vortex shedding, not between the displacement and lift force, and it has been shown by [6] that these two phases are not always the same. These difficulties mean a direct comparison between existing VIV and driven oscillation data has not been made at low Re .

This paper attempts to directly compare numerical VIV results with driven oscillation results at the same amplitude and frequency. Pure-tone driven oscillation is compared first, and then multi-harmonic forcing is used where discrepancies between the VIV and pure-tone driven oscillations exist. The improvement in the lift force history is shown, and the advantages and drawbacks of using multi-harmonic driven oscillation to model VIV are discussed.

Computational method

A two-dimensional, spectral-element method based on an accelerated frame of reference was used for this study. A 508 macro-element, non-deforming mesh was employed, with tensor-product 8th-order Lagrangian interpolation polynomials employed within each macro-element. Details of the method used can be found in [15]. A grid resolution study was performed using the stationary cylinder base case as the benchmark solution to check convergence. The resolution was altered by incrementing the order of the interpolation polynomials. No variation was observed in the value of the Strouhal number, St , as the polynomial order increased past 8, indicating the grid resolution was adequate.

Results

Vortex-Induced Vibrations

A set of simulations of flow past an elastically-mounted cylinder was run to determine the VIV response. As in low- Re experiments, three amplitude response branches were observed; the initial, upper, and trailing branches. The branches are defined in

figure 2a. The upper branch was the largest amplitude response branch, with amplitudes up to $A^* \simeq 0.5$. The upper branch also coincided with the range of U^* over which synchronisation of the primary response frequency f and the natural structural frequency f_N occurred.

The initial branch was characterised by a sharp increase in A^* with increasing U^* . While the main response frequency f was close to the vortex shedding frequency of the stationary cylinder f_V , a number of frequency components were present, with the displacement showing significant beating over time.

The trailing branch occurred at values of U^* higher than the synchronisation range. It exhibited low amplitudes of response, and so the frequency $f \simeq f_V$. These response results are presented in figure 2a and b.

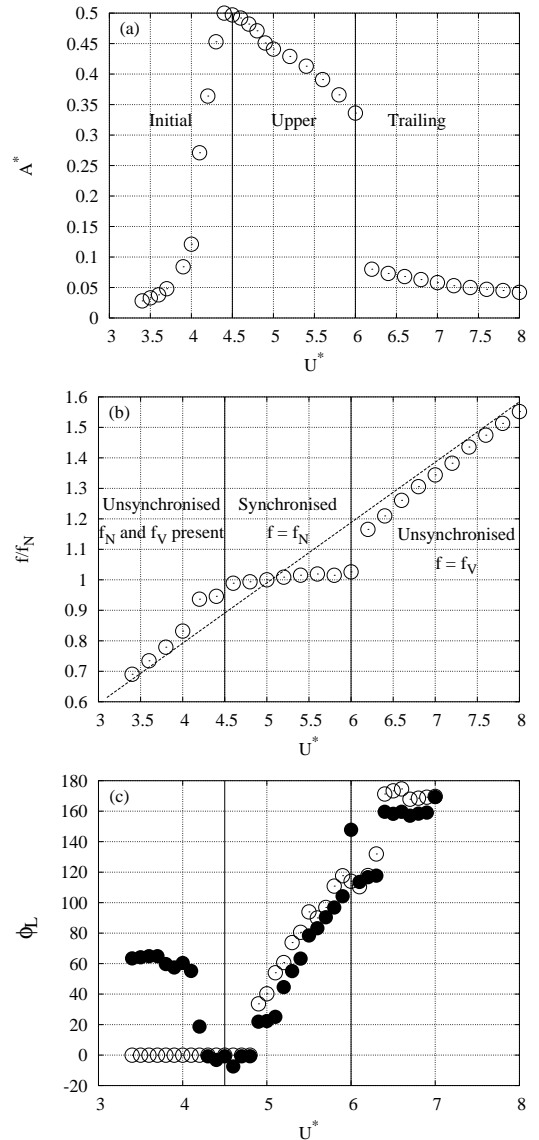


Figure 2: Response of the elastically-mounted cylinder. (a) Amplitude response. (b) Frequency response. $\circ f/f_N$, - - - f_V/f_N (c) Phase between lift force and displacement; \circ Elastically-mounted cylinder, \bullet Pure-tone driven cylinder.

Shown in figure 2c are the phase characteristics of this system. Phase was defined as the lag that produced the greatest correlation coefficient, obtained by calculating the cross-correlation between the lift force and displacement. Similar to the high-

Re experimental studies, the phase changed between approximately 0° and 180° over the range of significant response. However, unlike the high-*Re* experiments, which see the phase change as a sudden jump, this change is an almost linear climb over the upper branch, with smaller jumps at the initial-upper and upper-trailing transitions.

Pure-Tone Driven Oscillation

To investigate the effectiveness of modelling VIV with driven oscillation, pure-tone driven oscillation simulations were performed at the amplitude and frequencies obtained during the elastically-mounted simulations for a direct comparison. Where the amplitude of response in the VIV case was not steady, the maximum amplitude was used.

The phase of these simulations are compared directly to the VIV phase in figure 2c. It is shown that the phase characteristics of the two set-ups are very similar over the upper branch, especially for $U^* \geq 5.0$. Large discrepancies in phase exist throughout the initial branch, even though the amplitude of oscillation is only small, $O\{0.05D\}$. Interestingly, the phase results from the pure-tone oscillation match the VIV results closely over the initial-upper transition, even though many frequency components are present during VIV in this region. However, pure-tone driven oscillation cannot capture all the characteristics of VIV in this region, due to the high levels of modulation of cylinder oscillation. The largest oscillations also occur in this region, highlighting the importance of the development of multi-frequency models.

Multi-Frequency Driven Oscillation

Three cases were selected for multi-frequency driven oscillation testing. A case matching VIV at $U^* = 4.0$ was selected as a large discrepancy in ϕ_L existed between the VIV and pure-tone driven oscillation at these conditions. It was also observed that two significant frequencies existed in the VIV response of the cylinder at these conditions, f_V and f_N .

The second case selected was at $U^* = 4.6$. The largest amplitude oscillations occurred here, hence the importance of an accurate model. Significant beating was also evident in the displacement history, indicating the influence of more than one frequency.

The third case selected was at $U^* = 5.0$. This case was chosen because the cylinder natural frequency was effectively equal to the vortex-shedding frequency from a stationary cylinder, $f_N = f_V$.

The frequencies to include at $U^* = 4.0$ and $U^* = 4.6$ were deduced by performing an FFT on the VIV response data. To determine the magnitude of each component, all other components except for the one of interest were filtered out in the frequency domain, and the filtered data transformed back to the time domain with an inverse FFT.

For the $U^* = 5.0$ case, an FFT was performed on the lift force data, as the second component of oscillation was too small to be detected through FFT analysis of the response. The magnitude of each force component was deduced in the same fashion as the response components at $U^* = 4.0$. The linear equation of motion, $m\ddot{y} + c\dot{y} + ky = F$, was then solved for each force component, to establish the magnitude of each response component. The input frequencies and respective displacement amplitudes are presented in table 1.

The lift force and phase for the multi-frequency cases are presented in table 2, along with the corresponding VIV and pure-tone driven oscillation results. The values reported were taken

U^*	f_1	A_1^*	f_2	A_2^*	f_3	A_3^*
4.0	0.206	0.086	0.230	0.014	-	-
4.6	0.216	0.302	0.209	0.101	0.221	0.101
5.0	0.200	0.491	0.600	0.003	-	-

Table 1: The input parameters for the two multi-frequency driven oscillation cases.

from the steady-state portion of the response in each case.

Simulation	$U^* = 4.0$	$U^* = 4.6$	$U^* = 5.0$
	Peak lift coefficient, C_{LMAX}		
VIV	1.22	2.476	0.246
Pure-Tone	1.01	0.682	0.266
Multi-Frequency	1.03	2.681	0.208
Phase, ϕ_L			
VIV	0.70	-0.78	42.50
Pure-Tone	60.61	20.69	22.32
Multi-Frequency	58.93	-0.77	46.25

Table 2: Maximum lift coefficient and phase for the multi-frequency driven oscillation cases, compared to the corresponding pure-tone and VIV cases. It can be seen that the extra components added at $U^* = 4.6$ have a very significant effect on C_{LMAX} .

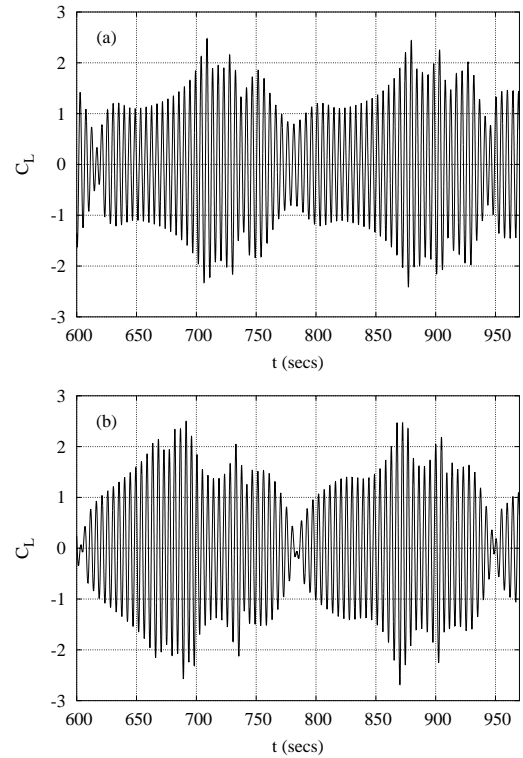


Figure 3: History of the lift force experienced by the cylinder at $U^* = 4.6$ (a) VIV. (b) Multi-frequency driven oscillation using the primary and two secondary frequency components of the VIV case. The agreement is close, but not perfect.

It can be seen from the values in table 2 that the multi-frequency oscillations have a varying degree of impact compared to pure-tone oscillations. The largest difference between the multi-frequency and pure-tone oscillations occurs in the initial branch and the initial-upper transition region, where extra frequency components are clearly present during VIV.

For $U^* = 4.0$, the value of C_{LMAX} for pure-tone and multi-

frequency oscillation was similar, but the multi-frequency case displayed significant beating, and was a much more accurate recreation of the VIV case. The maximum lift coefficient, C_{LMAX} , from the multi-frequency oscillation at $U^* = 4.6$, matched the VIV case closely, and was markedly better than the pure-tone case. The lift coefficient also showed a constant beating over time, that was not completely regular. A similar phenomenon occurred during VIV. This is illustrated in figure 3.

The phase results obtained were encouraging, but more work is required before any significant conclusions can be drawn from them. While there seems to be a very close agreement between the phase results taken from VIV and multi-frequency oscillation at $U^* = 4.6$, they are both negative, which is not expected for a positive energy transfer. Also, the results at $U^* = 5.0$ indicate the extra frequency component makes the phase vary by approximately 20° . Obtaining phase by cross-correlation is heavily dependent on the accuracy of the frequency of the driving signal, so a discrepancy of this magnitude is not unexpected.

Conclusions

While pure-tone driven oscillation captures many of the features of VIV, it has been shown that it misses some significant effects, especially in the region where the largest oscillations occur. It is for this reason that a more complete model for VIV has been investigated, namely one that includes extra frequency components.

Specific examples from the initial and upper branches of response have been examined. It was discovered that in the initial branch, at the equivalent of $U^* = 4.0$, adding a secondary frequency component to a driven oscillation changed the maximum amplitude of the lift force very little. However, it had the effect of making the lift force history much more similar to the VIV case it was to model.

However, at $U^* = 4.6$, adding extra frequency components had a significant effect on the maximum lift coefficient obtained, when compared to the pure-tone oscillation. This lift coefficient was also much closer to the VIV case lift coefficient. This result is important as it shows the magnitude of the lift force is not solely dependent on the peak amplitude of oscillation, but can also be dependent on the oscillation history.

At $U^* = 5.0$ where $f_N = f_V$, adding the small extra frequency component had very little effect on the lift force magnitude. Over the range $5.0 < U^* < 6.0$, the cylinder oscillation appears to be a pure-tone oscillation, and it is concluded that a pure-tone driven oscillation in this region is sufficient for the modelling of VIV.

Adding the extra component had little effect on the phase angle in either case, with both still differing when compared to their corresponding VIV cases, except at $U^* = 4.6$. However, the sensitivity of the response to minor changes in forcing indicate that to accurately predict the phase difference may require an exceptionally accurate representation of the forcing signal.

It has been shown that multi-frequency driven oscillation offers an improvement over pure-tone oscillation in modelling VIV, especially in the region of largest oscillations. It is envisaged that further work of this nature will lead to a better understanding of the nature of VIV, and an improved capability to predict it.

Acknowledgements

Primary support for this research program was provided by the Monash University Engineering research committee. Mr. Leoncini also acknowledges support from the Department of Me-

chanical Engineering, Monash University, through a Departmental Postgraduate Scholarship.

References

- [1] Anagnostopoulos, P. and Bearman, P., Response characteristics of a vortex-excited cylinder at low Reynolds numbers, *J. Fluids & Structures*, **6**, 1992, 39–50.
- [2] Blackburn, H., Govardhan, R. and Williamson, C., A complementary numerical and physical investigation of vortex-induced vibration, *J. Fluids & Structures*, **15**, 2000, 481–488.
- [3] Blackburn, H. and Henderson, R., A study of two-dimensional flow past an oscillating cylinder, *J. Fluid Mech.*, **1385**, 1999, 255–286.
- [4] Blackburn, H. and Karniadakis, G., Two- and three-dimensional simulations of vortex-induced vibration of a circular cylinder, in *Proceedings of the Third International offshore and polar engineering conference*, Singapore, 1993.
- [5] Carberry, J., *Wake states of a submerged oscillating cylinder and of a cylinder beneath a free surface*, Ph.D. thesis, Monash University, 2001.
- [6] Carberry, J., Sheridan, J. and Rockwell, D., Forces and wake modes of an oscillating cylinder, *J. Fluids & Structures*, **15**, 2001, 523–532.
- [7] Carberry, J., Sheridan, J. and Rockwell, D., Vortex forces on an oscillating cylinder, in *Proceedings of IMECE: ASME International Mechanical Engineering Congress and Exposition*, 2002, 1–7, 1–7.
- [8] Feng, C., *The measurement of vortex-induced effects in flow past a stationary and oscillating circular and D-section cylinders*, Master's thesis, University of British Columbia, 1968.
- [9] Govardhan, R. and Williamson, C., Modes of vortex formation and frequency response of a freely vibrating cylinder, *J. Fluid Mech.*, **420**, 2000, 85–130.
- [10] Khalak, A. and Williamson, C., Dynamics of a hydroelastic cylinder with very low mass and damping, *J. Fluids & Structures*, **10**, 1996, 455–472.
- [11] Khalak, A. and Williamson, C., Motions, forces and mode transitions in vortex-induced vibrations at low mass-damping, *J. Fluids & Structures*, **13**, 1999, 813–851.
- [12] Koopman, G., The vortex wakes of vibrating cylinders at low Reynolds numbers, *J. Fluid Mech.*, **28**, 1967, 501–512.
- [13] Sarpkaya, T., Fluid forces on oscillating cylinders, *Journal of the waterways, port, coastal and ocean division of ASCE*, **104**, 1978, 275–290.
- [14] Staubli, T., Calculation of the vibration of an elastically mounted cylinder using experimental data from forced oscillation, *J. Fluids Eng.*, **105**, 1983, 225–229.
- [15] Thompson, M., Hourigan, K. and Sheridan, J., Three-dimensional instabilities in the wake of a circular cylinder, *Experimental Thermal and Fluid Science*, **12**, 1996, 190–196.
- [16] Williamson, C. and Roshko, A., Vortex formation in the wake of an oscillating cylinder, *J. Fluids & Structures*, **2**, 1988, 355–381.